Distinct interleukin-6 production in IPL and TAFRO subtypes of idiopathic multicentric Castleman disease

Asami Nishikori,[1] Midori Filiz Nishimura,[1] Yoshito Nishimura,[2] Rio Yamada,[1] Tomoka Haratake,[1] Daisuke Ennishi,[3,4] Ryota Chijimatsu,[3] Toshihiro Ito,[5] Tomohiro Koga,[6] Sayaka Ochi,[1] Yuri Kawahara,[1] Himawari Ueta,[1] Yudai Takeda,[1] Michael V. Gonzalez,[7] David C. Fajgenbaum,[7,8] Frits van Rhee,[9] Shuji Momose[10] and Yasuharu Sato[1*]

[1]Department of Molecular Hematopathology, Okayama University Graduate School of Health Sciences, Okayama, Japan; [2]Division of Hematology/Oncology, Mayo Clinic, Rochester, MN, USA; [3]Center for Comprehensive Genomic Medicine, Okayama University Hospital, Okayama, Japan; [4]Department of Hematology and Oncology, Okayama University Hospital, Okayama, Japan; [5]Department of Immunology, Nara Medical University, Nara, Japan; [6]Department of Immunology and Rheumatology, Nagasaki University Graduate School of Biomedical Sciences, Nagasaki, Japan; [7]Center for Cytokine Storm Treatment & Laboratory, Department of Medicine, Perelman School of Medicine, University of Pennsylvania, Philadelphia, PA, USA; [8]Castleman Disease Collaborative Network, Philadelphia, PA, USA; [9]University of Arkansas for Medical Sciences, Little Rock, AR, USA and [10]Department of Pathology, Saitama Medical Center, Saitama Medical University, Saitama, Japan

Correspondence: Y. Sato
satou-y@okayama-u.ac.jp

Received: May 6, 2025.
Accepted: August 29, 2025.
Early view: September 11, 2025.

https://doi.org/10.3324/haematol.2025.288147

Abstract

Idiopathic multicentric Castleman disease (iMCD) is a rare lymphoproliferative disorder characterized by systemic inflammation and lymphadenopathy. Two major clinical subtypes, idiopathic plasmacytic lymphadenopathy (iMCD-IPL) and iMCD with thrombocytopenia, anasarca, fever, renal dysfunction/reticulin fibrosis, and organomegaly (iMCD-TAFRO), have distinct pathophysiological mechanisms. While interleukin-6 (IL-6) is known to be elevated in iMCD, differences in the sources of IL-6 production between subtypes remain unclear. We examined the source of IL-6 production and its transcriptional regulation across iMCD subtypes using immunohistochemistry, *in situ* hybridization, and gene expression profiling. Immunohistochemistry and *in situ* hybridization revealed that plasma cells were the predominant IL-6-expressing cells in iMCD-IPL, whereas vascular endothelial cells expressed IL-6 in iMCD-TAFRO. Plasma cells exhibited stronger IL-6 protein expression in iMCD-IPL than in iMCD-TAFRO. Gene expression analysis revealed upregulation of *XBP1, MZB1, DERL3, SSR4, FKBP11, FKBP2, PIM2, RABAC1*, and *SDF2L1* in iMCD-IPL, implicating endoplasmic reticulum stress and plasma cell differentiation in IL-6 dysregulation. Our findings suggest that *XBP1*-mediated IL-6 production may contribute to the pathogenesis of iMCD-IPL, potentially explaining its favorable responses to IL-6 blockade therapy. In contrast, IL-6 production in iMCD-TAFRO may be predominantly from vascular endothelial cells, suggesting that elevated serum IL-6 is a secondary phenomenon of the cytokine storm in this subtype. Future studies should clarify how proteomics and gene expression profiling could inform subtype-specific therapeutic strategies in iMCD.

Introduction

Idiopathic multicentric Castleman disease (iMCD) is a rare, non-clonal lymphoproliferative disorder characterized by systemic lymphadenopathy and inflammation.[1,2] Two clinical subtypes, iMCD with idiopathic plasmacytic lymphadenopathy (iMCD-IPL) and iMCD with thrombocytopenia, anasarca, fever, renal dysfunction/reticulin fibrosis, and organomegaly (iMCD-TAFRO), display distinct clinicopathological features and responses to treatment.[3,4] iMCD-IPL patients have an indolent clinical course, and exhibit plasmacytic lymph node histology and hypergammaglobulinemia. In contrast, iMCD-TAFRO is characterized by aggressive clinical symptoms with TAFRO features. Histologically, iMCD-TAFRO shows marked vascularization in atrophic germinal centers and the interfollicular area. Patients with iMCD-TAFRO often require intensive care unit admissions or renal replacement therapy. In addition, the high levels of inflammatory cytokines and gene expression patterns observed in iMCD-TAFRO suggest a pathological state of cytokine storm.[5,6]

While interleukin-6 (IL-6) inhibitors have been the first-

line treatment for iMCD over the past decade,[7] patients with different iMCD subtypes exhibit variable responses to treatment.[3,8,9] As previously reported, patients with iMCD-IPL usually have favorable responses to IL-6 blockade therapy with siltuximab or tocilizumab,[3,10] with sustained remissions over time.[11,12] However, patients with iMCD-TAFRO are more likely to show marginal responses to IL-6-directed therapy[13] and often require combined high-dose glucocorticoids, rituximab, or either lymphoma- or myeloma-based systemic chemotherapy.[3,14,15] Furthermore, there are reports that tumor necrosis factor (TNF) inhibitors and Bruton tyrosine kinase (BTK) inhibitors are effective.[16,17] The divergent treatment outcomes suggest underlying subtype-specific pathogenic differences, potentially related to the role of IL-6 and the cells producing it in each subtype.

Despite the differences in clinical responses, patients with iMCD-IPL and iMCD-TAFRO often exhibit similarly elevated serum IL-6 levels.[3,18] A recent study in Japanese cohorts revealed that one-quarter of patients with TAFRO symptoms do not have lymphadenopathy.[19] The pathological differences between TAFRO without lymphadenopathy and TAFRO with lymphadenopathy (including iMCD-TAFRO) remain unclear, but they may be due to differences in the expression of inflammation-related genes in the lymph nodes. Furthermore, a recent gene expression study revealed significant enrichment of the PI3K-Akt signaling pathway in iMCD-TAFRO, suggesting that non-IL-6 cytokines may be the primary disease driver of its pathogenesis.[20] Previous studies identified vascular endothelial cells or B cells as a source of IL-6 in iMCD lymph nodes, but did not compare subtypes.[21-24] Thus, the present study aimed to elucidate and compare the cellular sources of IL-6 and associated transcriptional regulators in iMCD-IPL and iMCD-TAFRO using immunohistochemistry, *in situ* hybridization, and gene expression analysis.

Methods

Patients and definitions of subtypes of idiopathic multicentric Castleman disease

Sixty-four patients with iMCD-IPL (N=50) or iMCD-TAFRO (N=14) were included in the study. All cases were retrieved from pathology consultation files at Okayama University, Japan, and met the diagnostic criteria for iMCD.[1] IgG4-related disease was ruled out in all cases based on established exclusion criteria.[25,26] Currently, three sets of diagnostic criteria are used for iMCD-IPL,[4,27-29] and these criteria differ slightly. In this study, iMCD-IPL was diagnosed according to the criteria defined by Kojima *et al.*, including: (i) prominent polyclonal hypergammaglobulinemia (gamma globulin >4.0 g/dL or serum IgG level >3,500 mg/dL), (ii) generalized lymphadenopathy, (iii) absence of definite autoimmune disease, and (iv) sheet-like infiltration of mature plasma cells.[28] There are several diagnostic criteria for iMCD-TAFRO,[30,31] and this study used the international definition[31] through which iMCD-TAFRO is diagnosed in those cases with iMCD-consistent lymph node pathology meeting at least four clinical criteria (thrombocytopenia, anasarca, fever/hyperinflammatory status, and organomegaly), in addition to supplementary criteria, including renal dysfunction, or pathological features in the bone marrow such as reticulin fibrosis or megakaryocyte hyperplasia.[31] Furthermore, histological subtypes of iMCD were classified based on international criteria.[13] All patients were serologically or immunohistochemically negative for Kaposi's sarcoma-associated herpesvirus/human herpesvirus 8. This study was approved by the Institutional Review Board of Okayama University (protocol number 2007-033) and was performed in accordance with the tenets of the Declaration of Helsinki.

Histology, immunohistochemistry, sample quantification, and *in situ* hybridization

All lymph node specimens were fixed in 10% formaldehyde and embedded in paraffin. Formalin-fixed paraffin-embedded (FFPE) tissue blocks were sliced into 3-µm thick sections and stained with hematoxylin and eosin. Immunohistochemical staining for IL-6 was performed in all cases, and H scores were calculated. Additionally, IL-6 and IL-6 receptor (IL-6R) mRNA expression was visualized in two iMCD-IPL and two iMCD-TAFRO cases (*Online Supplementary Appendix*).

Whole transcriptome analysis

Whole transcriptome analysis was performed on 20 Japanese patients with iMCD-IPL (N=12), iMCD-not otherwise specified (NOS) (N=6), and iMCD-TAFRO (N=2) with frozen lymph node lesions. Patients who did not meet the criteria for iMCD-IPL and iMCD-TAFRO criteria were defined as having iMCD-NOS.[6,20] However, all iMCD-NOS included in the study were iMCD-TAFRO-like cases that did not completely meet the criteria for iMCD-TAFRO, although they had pleural and/or ascites effusions and showed hypervascular histology. The details of the iMCD-NOS patients included in this study are summarized in *Online Supplementary Table S2*. Total RNA extraction and sequencing are described in the *Online Supplementary Appendix*. Following this, deconvolution analysis was performed using the abs mode of CIBERSORTx32 (*https://cibersortx.stanford.edu*) with transcripts per million values from whole transcriptome analysis.

Gene expression profiling

Gene expression profiling was performed using the nCounter platform (NanoString Technologies, Seattle, WA, USA) in 24 iMCD-IPL and seven iMCD-TAFRO cases with sufficient FFPE tissue that passed the RNA quality check. RNA extraction from FFPE tissue and analysis are described in the *Online Supplementary Appendix*.

Statistical analysis

For categorical data, we used the χ^2 test. The Wilcoxon rank sum test was used to compare two continuous variables. All *P* values were calculated using two-sided tests, and a threshold of 0.05 was used to measure statistical significance. Statistical analyses were performed using R version 4.2.1 (*https://cran.r-project.org*).

Results

Clinical findings

Table 1 summarizes the clinical characteristics of the patients in this study. There was no significant age difference between patients with iMCD-IPL or iMCD-TAFRO (*P*=0.644). Consistent with previous reports and subtype definitions, iMCD-IPL patients had higher platelet counts and immunoglobulin (IgG, IgA, IgM) levels than iMCD-TAFRO patients (*P*<0.001). Serum IL-6 levels were comparable between subtypes (*P*=0.234).

Histological, immunohistochemical, and *in situ* hybridization findings

Histological findings of the iMCD-IPL and iMCD-TAFRO cases are shown in Figures 1 and 2, respectively. iMCD-IPL lymph nodes showed normal to hyperplastic germinal centers with an expanded interfollicular area featuring sheet-like plasma cell proliferation (Figure 1A); hemosiderin deposition was frequently observed (Figure 1B). In contrast, iMCD-TAFRO lymph nodes had atrophic germinal centers with promi-

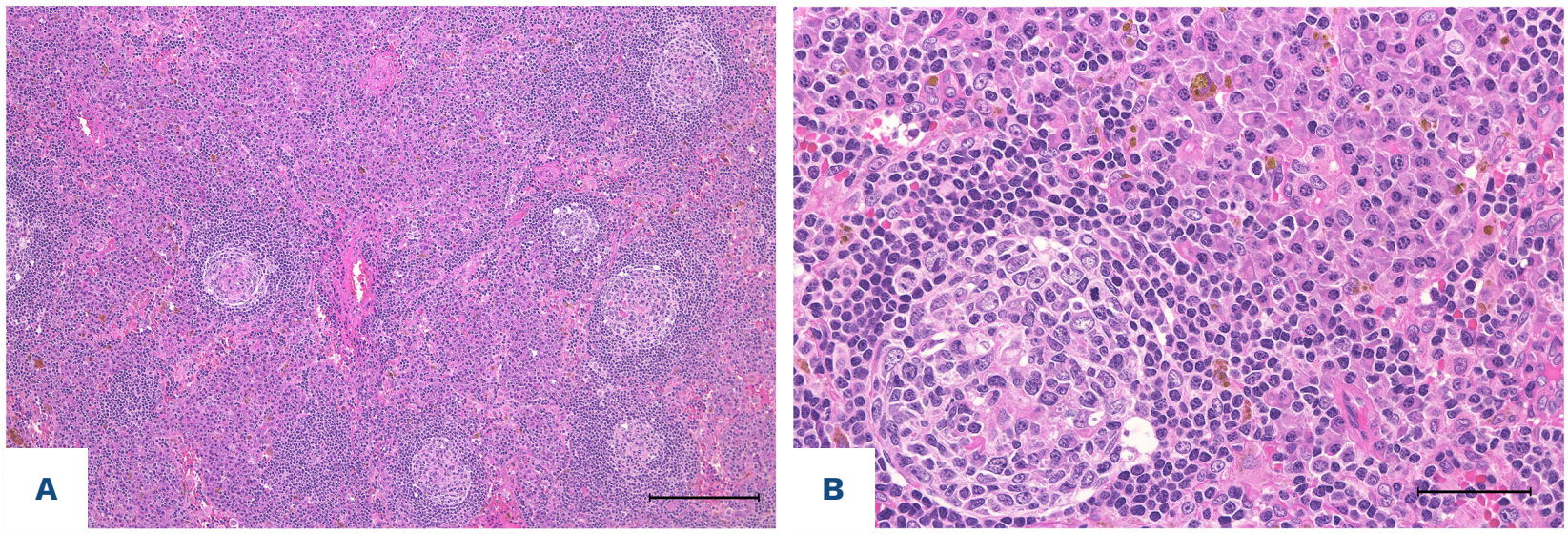

Figure 1. Histopathological features of idiopathic multicentric Castleman disease-idiopathic plasmacytic lymphadenopathy (iMCD-IPL). (A) Interfollicular areas are expanded, and germinal centers show normal to hyperplastic features. Scale bar = 200 μm. (B) Sheet-like proliferation of mature plasma cells in the interfollicular areas and hemosiderin deposition. Scale bar = 50 μm.

Table 1. Comparison of clinical findings between subtypes of idiopathic multicentric Castleman disease.

Findings	iMCD-IPL N=50	iMCD-TAFRO N=14	*P*
Age, years, median (IQR)	54.0 (62.0-44.5)	49.0 (65.5-41.8)	0.644
Sex, male/female, N	27/23	11/3	-
Laboratory findings,* median (IQR)			
WBC, $\times10^3/\mu L$, N=43	8.0 (9.6-5.7)	9.0 (12.4-5.7)	0.456
Platelets, $\times10^3/\mu L$, N=56	387 (439-286)	35 (54-22)	<0.001
Hemoglobin, g/dL, N=57	10.3 (11.5-9.1)	9.0 (11.3-7.5)	0.269
CRP, mg/dL, N=55	6.5 (8.8-3.4)	6.0 (16.1-1.9)	0.992
Serum IL-6, pg/mL, N=16	37.5 (52.5-23.6)	15.6 (26.6-10.7)	0.234
IgG, mg/dL, N=52	4,727.0 (6,014.5-4,274.3)	1,317.7 (1,560.3-1,193.1)	<0.001
IgM, mg/dL, N=41	215.0 (271.2-154.0)	73.7 (96.3-63.0)	<0.001
IgA, mg/dL, N=41	553.6 (686.0-450.0)	188.6 (227.3-169.0)	<0.001

Significance was calculated using the Mann-Whitney U test, with *P* values <0.001 considered statistically significant. *Normal ranges: white blood cells, $3.3\text{-}8.6\times10^3/\mu L$; platelets, $158\text{-}348\times10^3/\mu L$; hemoglobin, 13.7-16.8 g/dL (male), 11.6-14.8 g/dL (female); C-reactive protein, 0.00-0.30 mg/dL; interleukin-6, 0.0–4.0 pg/mL; IgG, 870-1,700 mg/dL; IgM, 31-200 mg/dL (male), 52-270 mg/dL (female); IgA, 110-410 mg/dL. iMCD-IPL: idiopathic multicentric Castleman disease with idiopathic plasmacytic lymphadenopathy; iMCD-TAFRO: idiopathic multicentric Castleman disease with thrombocytopenia, anasarca, fever, renal dysfunction/reticulin fibrosis, and organomegaly; IQR: interquartile range; WBC: white blood cells; CRP: C-reactive protein; IL-6: interleukin 6; Ig: immunoglobulin.

nent vascular proliferation (Figure 2A). "Whirlpool" vessels often appeared within the atrophic germinal centers (Figure 2B). iMCD-TAFRO cases also showed variable degrees of plasmacytosis; some cases had extensive plasma cell proliferation alongside marked vascularity. In iMCD-TAFRO, plasma cells are not arranged in sheet-like formations but are interspersed among proliferating blood vessels and lymphocytes (Figure 2C, D).

Immunohistochemistry for IL-6 showed significantly stronger IL-6 protein staining in iMCD-IPL than in iMCD-TAFRO (Figure 3). In iMCD-IPL, the interfollicular zones contained sheet-like mature plasma cell proliferation (Figure 3A) with granular cytoplasmic IL-6 staining (Figure 3C). Vascular endothelial cells in iMCD-IPL were also IL-6-positive, although less intensely than the plasma cells (Figure 3E). In iMCD-TAFRO, some cases demonstrated interfollicular plasmacytosis (Figure 3B) with IL-6-positive plasma cells (Figure 3D), and IL-6 staining was likewise seen in vascular endothelial cells (Figure 3F). Quantitatively, the IL-6 H-score was significantly higher in iMCD-IPL than in iMCD-TAFRO (P<0.001) (Figure 3G).

In situ hybridization corroborated the immunohistochemistry results: IL-6 mRNA signals appeared primarily in plasma cells in iMCD-IPL, whereas in iMCD-TAFRO, they were detected in vascular endothelial cells (Figure 4A, B). Additionally, in iMCD-IPL, we observed slight signals in vascular endothelial cells compared to those in plasma cells (*Online Supplementary Figure S1*). Similarly, IL-6R mRNA was localized to plasma cells in iMCD-IPL and endothelial cells in iMCD-TAFRO (Figure 4C, D).

Whole transcriptome analysis

The results of the whole transcriptome analysis showed a correlation of transcripts per million between iMCD cases (Figure 5). Notably, several iMCD-IPL samples (IPL1, 2, 4, 5, 6, 8) clustered tightly together along with one iMCD-NOS and one iMCD-TAFRO case (NOS1 and TAFRO2), whereas the remaining iMCD-IPL cases (IPL3, 7, 9, 10, 11, 12) fell into separate clusters. All iMCD-IPL cases classified in the separate clusters showed a distribution value of fragments ≥200 nucleotides (DV200) of less than 95%. Non-hierarchical cluster analysis was performed to identify the upregulat-

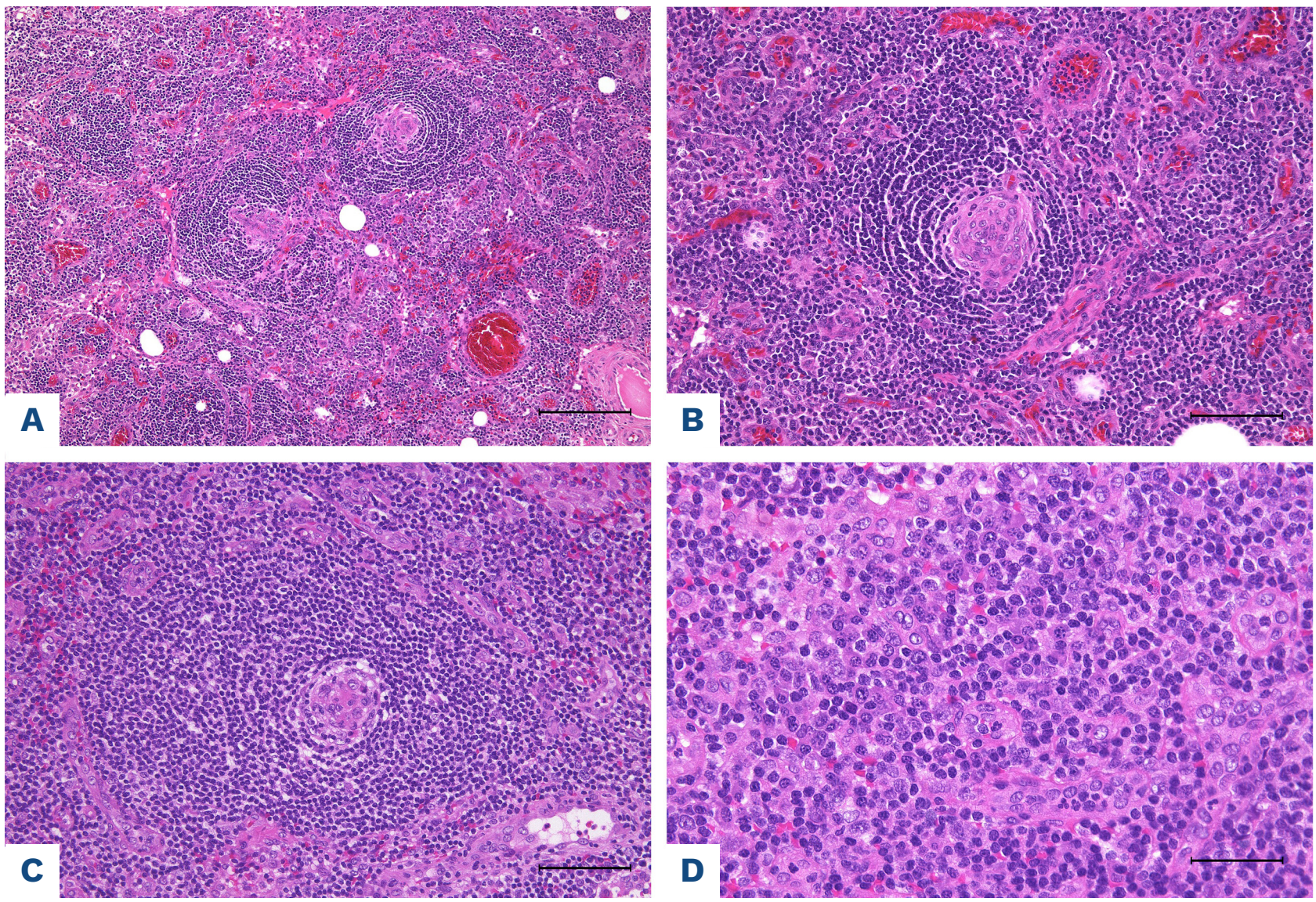

Figure 2. Histopathological features of idiopathic multicentric Castleman disease with thrombocytopenia, anasarca, fever, renal dysfunction/reticulin fibrosis, and organomegaly (iMCD-TAFRO). (A, B) iMCD-TAFRO without plasmacytosis. Atrophic germinal centers and severe vascularization. Scale bar = 200 μm (A). Proliferation of whirlpool vessels within the germinal centers. Scale bar = 100 μm. (B). (C, D) iMCD-TAFRO with plasmacytosis. An atrophic germinal center with a whirlpool vessel. Scale bar = 100 μm (C). In the interfollicular area, prominent vascular proliferation and plasma cells admixed with lymphocytes can be seen. Scale bar = 50 μm (D).

ed genes in these case groups. Focusing on the dominant iMCD-IPL cluster, we identified 105 genes significantly up-regulated in iMCD-IPL (*Online Supplementary Figure S2*). By contrast, clustering of the 105 genes showed a mixed gene expression pattern in iMCD-TAFRO and iMCD-NOS cases. The 105 genes included plasma cell-related genes such as *XBP1* and *MZB1*. Considering the possibility that the gene signature characteristic of iMCD-IPL depends on the amount of plasma cells in the constituent cells, we performed deconvolution analysis (*Online Supplementa-*

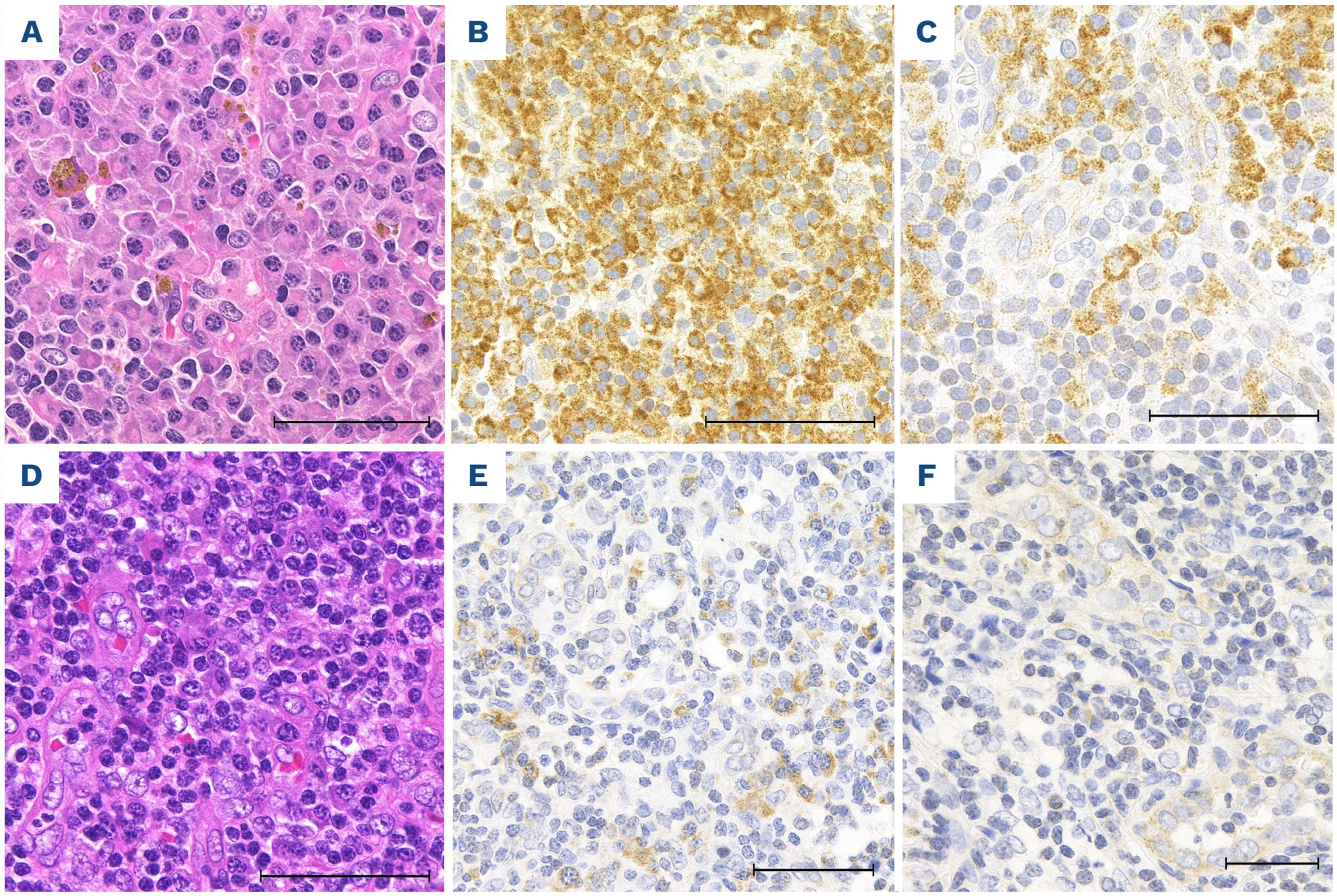

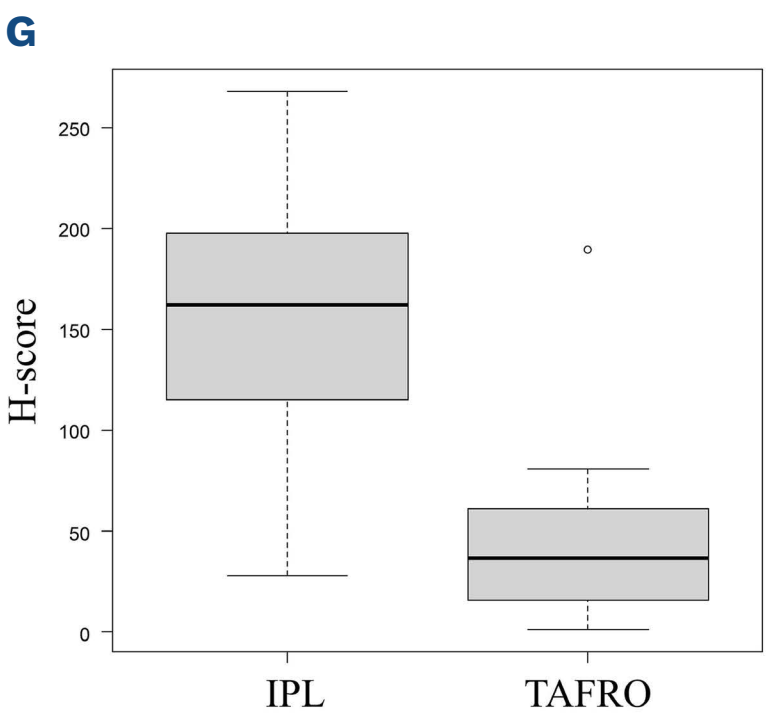

Figure 3. Interleukein-6 immunohistochemical staining in idiopathic multicentric Castleman disease subtypes. (A) Idiopathic multicentric Castleman disease-idiopathic plasmacytic lymphadenopathy (iMCD-IPL). Sheet-like proliferation of mature plasma cells in the interfollicular area. Scale bar = 50 μm. (B) Idiopathic multicentric Castleman disease with thrombocytopenia, anasarca, fever, renal dysfunction/reticulin fibrosis, and organomegaly (iMCD-TAFRO). Marked vascularization with plasmacytosis in the interfollicular area. Scale bar = 100 μm. (C) Interleukin-6 (IL-6) immunostaining in iMCD-IPL. The cytoplasm of the plasma cells in the interfollicular area shows a granular staining pattern. Scale bar = 50 μm. (D) iMCD-TAFRO. IL-6 protein expression was detected in plasma cells, weaker than in iMCD-IPL. Scale bar = 50 μm. (E) Vascular endothelial cells in iMCD-IPL show weaker IL-6 protein expression than plasma cells. Scale bar = 50 μm. (F) iMCD-TAFRO. IL-6 protein expression was detected in the cytoplasm of vascular endothelial cells. Scale bar = 50 μm. (G) Comparison of IL-6 H-score between iMCD-IPL and iMCD-TAFRO. The IL-6 staining pattern was calculated on a four-point scale (0-3). The H-score was calculated for cell staining using the following formula: H-score = (% at 0) × 0 + (% at 1+) × 1 + (% at 2+) × 2 + (% at 3+) × 3, as described previously.[33] The IL-6 H-score was significantly higher in the iMCD-IPL group (P<0.001). iMCD-IPL: median (interquartile range): 162.1 (115.7-196.0); iMCD-TAFRO: median (interquartile range): 36.4 (17.7-58.3).

ry Figure S3). As a result, no significant difference in the amount of plasma cells was observed between iMCD-IPL and iMCD-TAFRO (*P*=0.536).

Gene expression profiling

Targeted gene expression profiling (nCounter) was performed on all available cases for the 105 genes to validate the RNA-sequencing findings. The top ten most highly expressed genes across all samples were *IGLL5, XBP1, MZB1, DERL3, SSR4, FKBP11, PIM2, FKBP2, RABAC1*, and *SDF2L1* (*Online Supplementary Figure S4*). Notably, nine of these genes (*XBP1, MZB1, DERL3, SSR4, FKBP11, FKBP2, PIM2, RABAC1,* and *SDF2L1*) were expressed at significantly higher levels in iMCD-IPL than in iMCD-TAFRO (*P*<0.05 for each with varying levels of significance as shown) (Figure 6). The rank order of gene expression by subtype is shown in *Online Supplementary Figure S5*.

Discussion

The present study provides the first direct evidence of differential pathways of IL-6 production between iMCD-IPL and iMCD-TAFRO, as determined through immunohistochemistry, *in situ* hybridization, and gene expression analysis. This report describes the first direct evidence of distinct IL-6 production mechanisms in iMCD-IPL *versus* iMCD-TAFRO. Previous reports noted IL-6 signaling in iMCD endothelial cells but did not differentiate between subtypes.[21,23] We found that IL-6 production by vascular endothelial cells is far more prominent in the iMCD-TAFRO subtype. In iMCD-TAFRO, we observed activation of the PI3K-Akt pathway and upregulation of cytokine storm-related genes such as *TNFA, IL1R, MTOR*, and *VEGFA*;[6,19] however, no significant difference in *IL6* gene expression was observed. Therefore, the elevation of serum IL-6 in iMCD-TAFRO is suggested to be a consequence of the subsequent cytokine storm rather than a primary disease driver.[5,34,35]

In contrast, in iMCD-IPL, we detected IL-6 protein, as well as IL-6 and IL-6R mRNA, within the proliferating plasma cells, supporting the hypothesis of autocrine IL-6 production. Notably, the gene expression data showing high *XBP1* in iMCD-IPL further reinforces an autocrine and possibly a paracrine mechanism, as *XBP1* is known to drive IL-6 secretion (Figure 7). *XBP1* is a transcription factor implicated in multiple myeloma, in which it enhances IL-6 secretion,

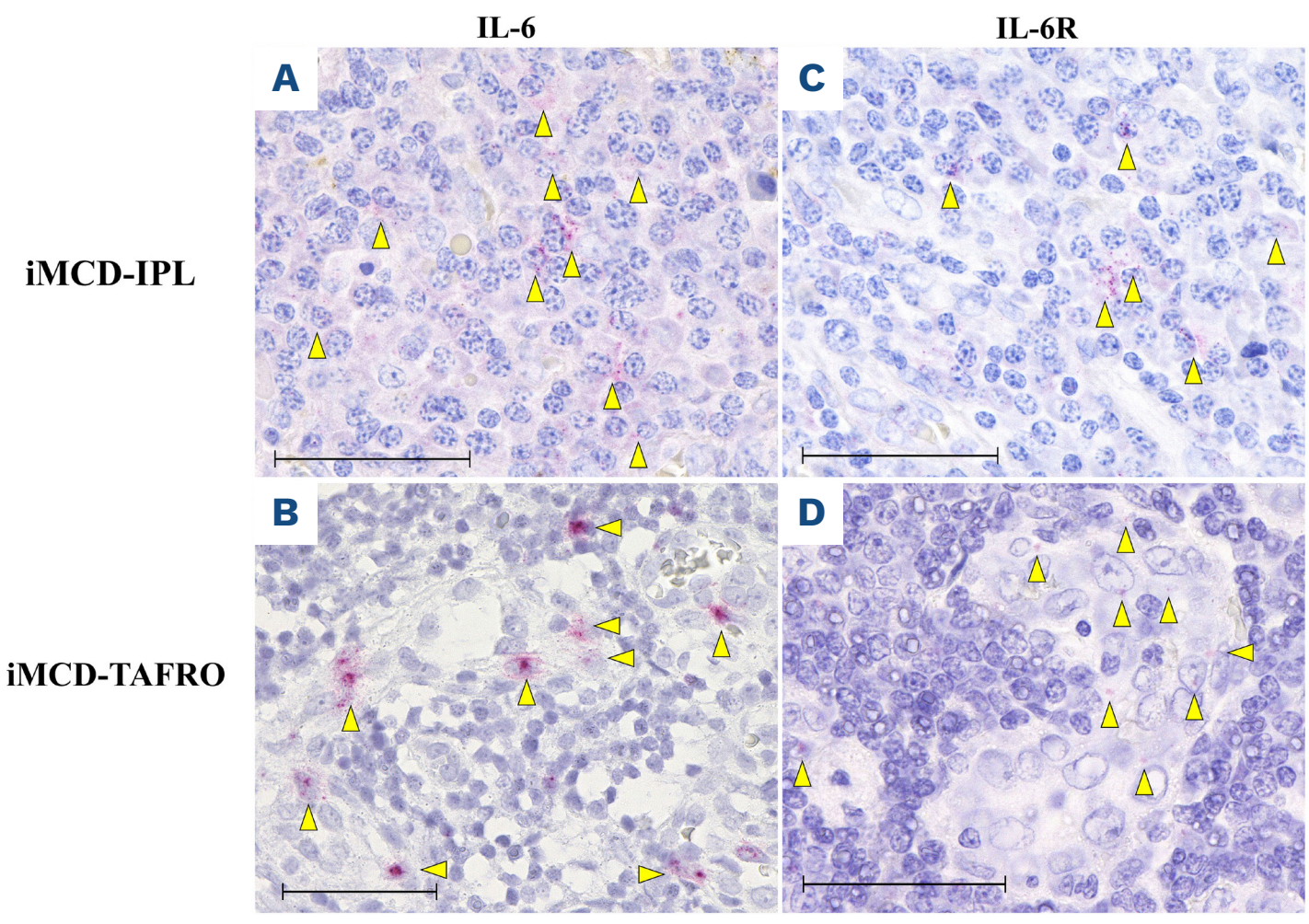

Figure 4. Interleukin-6 and interleukin-6 receptor *in situ* hybridization in idiopathic multicentric Castleman disease subtypes. (A) Idiopathic multicentric Castleman disease-idiopathic plasmacytic lymphadenopathy (iMCD-IPL). Interleukin-6 (IL-6) mRNA signals were observed mainly in plasma cells (yellow arrowheads). Scale bar = 50 μm. (B) Idiopathic multicentric Castleman disease with thrombocytopenia, anasarca, fever, renal dysfunction/reticulin fibrosis, and organomegaly (iMCD-TAFRO). IL-6 mRNA signals were detected in vascular endothelial cells (yellow arrowheads). No IL-6 mRNA signals were detected in the plasma cells. Scale bar = 50 μm. (C) iMCD-IPL. IL-6 receptor (IL-6R) mRNA signals were detected mainly in plasma cells (yellow arrowheads). Scale bar = 50 μm. (D) iMCD-TAFRO. IL-6R mRNA signals were observed in vascular endothelial cells (yellow arrowheads). No IL-6R mRNA signals were detected in the plasma cells. Scale bar = 50 μm.

plasma cell survival, and angiogenesis.[36-38] Furthermore, *XBP1* is an endoplasmic reticulum (ER) stress-related gene, and its expression is enhanced during the differentiation of B cells into plasma cells in lymph nodes.[36,39] Given that vascular proliferation is not considerably pronounced in iMCD-IPL,[20] *XBP1* activation in iMCD-IPL may likely be driv-

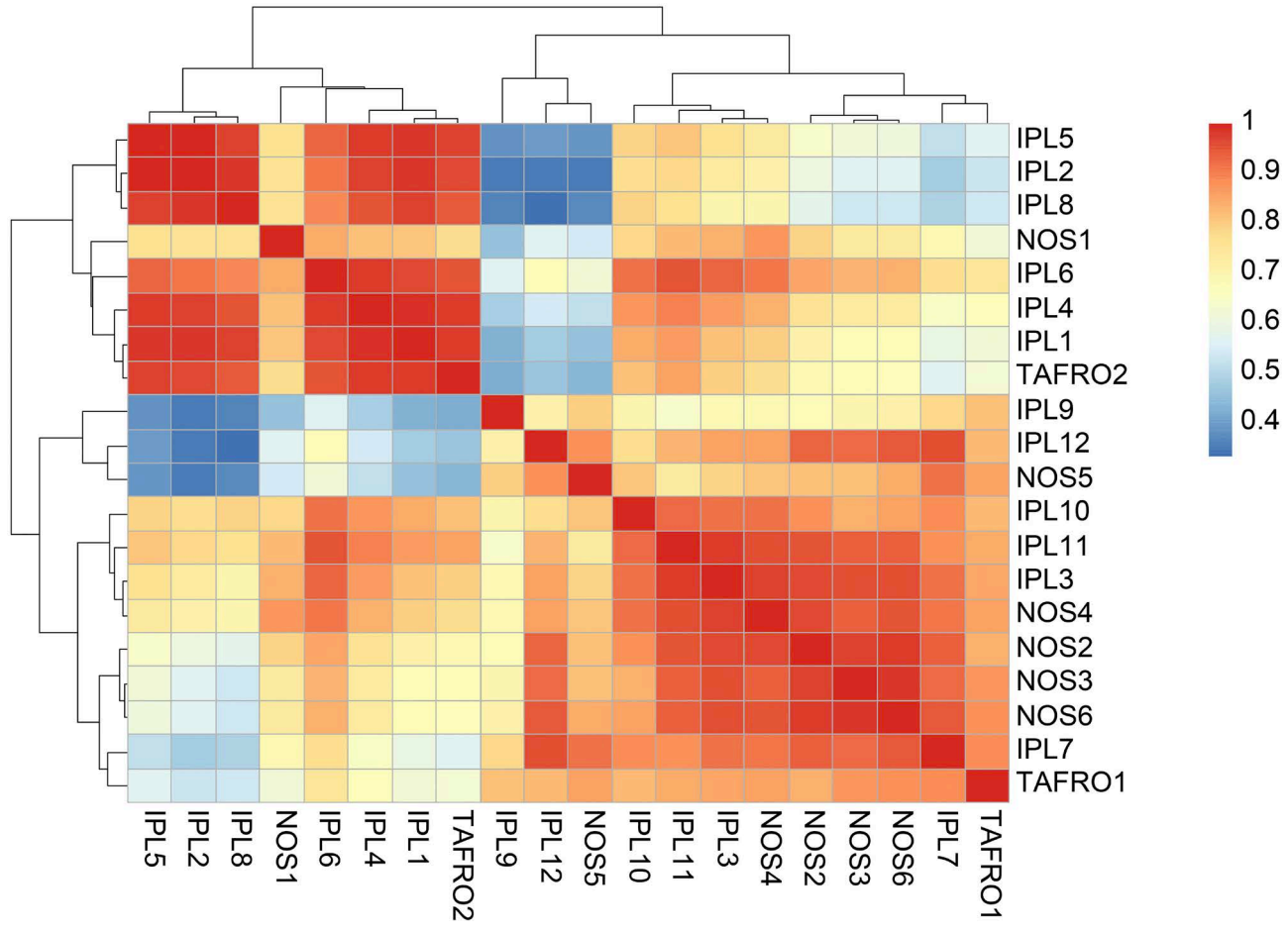

Figure 5. Whole transcriptome analysis in idiopathic multicentric Castleman disease subtypes. Correlation analysis between cases of idiopathic multicentric Castleman disease based on transcripts per million using 750 highly variable genes. Strong positive correlations were observed in the cluster containing IPL1, 2, 4, 5, 6, 8, NOS1, and TAFRO2.

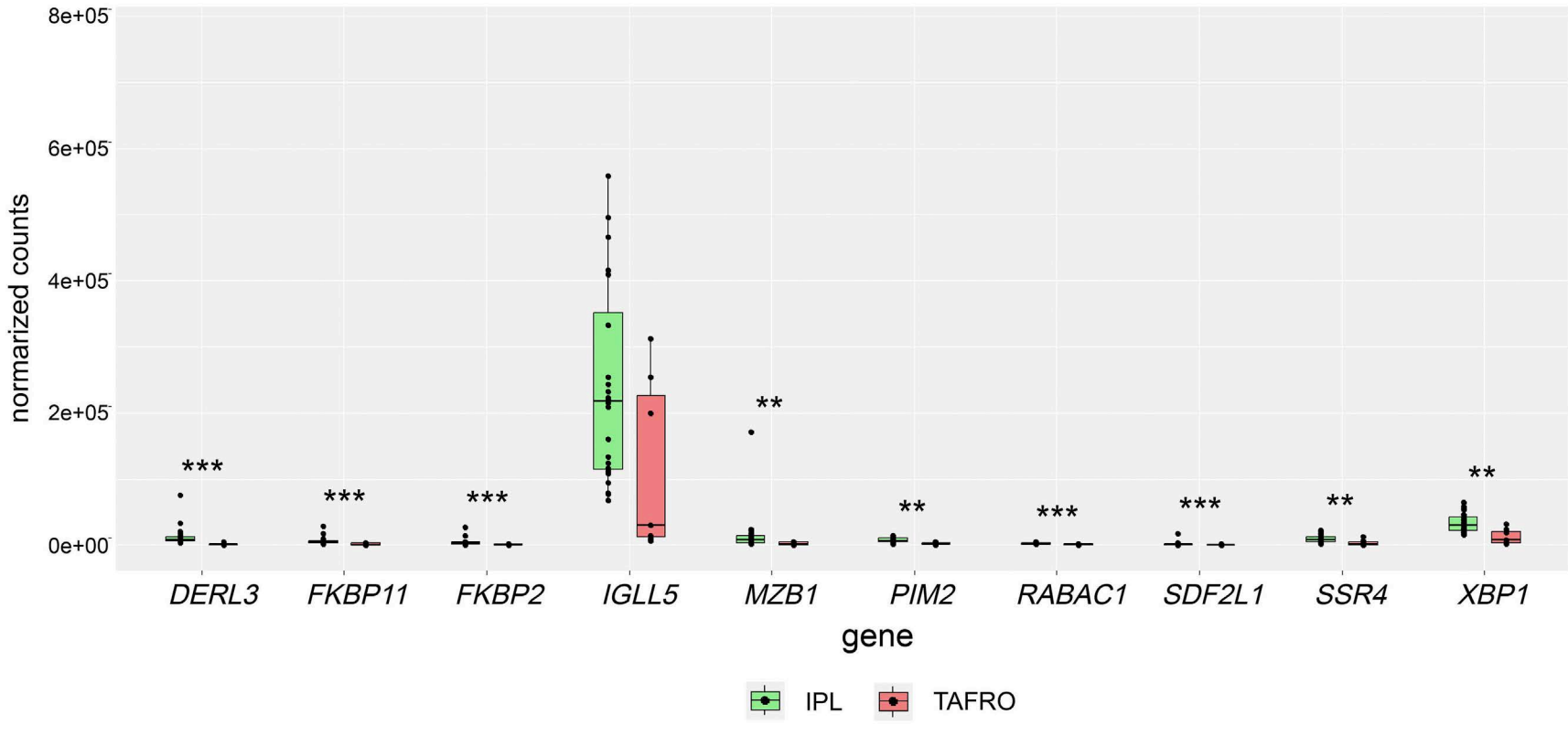

Figure 6. Gene expression analysis in idiopathic multicentric Castleman disease subtypes using a custom panel. Comparison of expression levels between idiopathic multicentric Castleman disease-idiopathic plasmacytic lymphadenopathy (iMCD-IPL) and idiopathic multicentric Castleman disease with thrombocytopenia, anasarca, fever, renal dysfunction/reticulin fibrosis, and organomegaly (iMCD-TAFRO) for the top ten expressed genes (*IGLL5, XBP1, MZB1, DERL3, SSR4, FKBP11, PIM2, FKBP2, RABAC1*, and *SDF2L1*). **P*<0.05, ***P*<0.01, ****P*<0.001, NS: not significant.

en by factors other than angiogenesis, consistent with an alternative mechanism of IL-6 upregulation in this subtype. The constitutive, *XBP1*-driven IL-6 cycle may explain clinical features in iMCD-IPL patients, including hypergammaglobulinemia and thrombocytosis. While the role of *XBP1* in promoting plasma cell survival may also contribute to the chronic nature of iMCD-IPL, further investigation is needed to identify the trigger for *XBP1* activation that leads to excessive plasma cell differentiation and IL-6 production. Furthermore, gene expression analysis in this study revealed that iMCD-IPL was associated with increased expression of ER stress-related genes, including *XBP1*. ER stress is closely related to plasma cells in lymph nodes, and it is crucial to determine whether the enhancement of this gene signature is dependent on the component cells of iMCD-IPL and iMCD-TAFRO. Deconvolution analysis revealed no significant difference in the estimated number of plasma cells between iMCD-IPL and iMCD-TAFRO, suggesting that the difference in IL-6 activity between the two groups may be attributed to their distinct characteristics rather than the quantity of plasma cells. Histologically, plasma cells in iMCD-TAFRO were observed to be mixed with vascular cells and lymphocytes, in contrast to the sheet-like proliferation observed in iMCD-IPL. The distribution areas and appearance patterns of plasma cells in iMCD-IPL and iMCD-TAFRO are considered to be different.

We noted that IL-6 protein staining in iMCD-IPL was markedly stronger in plasma cells than in vascular endothelial cells. Additionally, IL-6 staining was more intense in plasma cells in iMCD-IPL than in iMCD-TAFRO. The discrepancy likely does not reflect the sheer overproduction of IL-6, but rather that intracellular, autocrinally produced IL-6 is retained within iMCD-IPL plasma cells, rather than being secreted. Such a chronic autocrine IL-6 signaling mechanism could sustain ongoing plasma cell proliferation and related symptoms in iMCD-IPL, which needs to be verified in future studies. Conversely, the predominance of endothelial-derived IL-6 in iMCD-TAFRO may reflect a different pathophysiology and explain why IL-6 inhibitors have limited efficacy in some patients with iMCD-TAFRO. It is worth noting that immunohistochemically determined IL-6 H-scores were significantly higher in iMCD-IPL; one may need to consider that this could be influenced by the greater number of plasma cells in iMCD-IPL tissues, which may not truly reflect the actual amount of IL-6. However, as most iMCD-TAFRO cases did have various degrees of plasmacytosis with weak IL-6-positive cells, and we quantified H-scores in hotspots for each case, differences in staining intensity likely account for the higher H-scores in iMCD-IPL. We found similarly high *IGLL5* expression in both iMCD-IPL and iMCD-TAFRO, but the significance of this observation may differ by subtype. In iMCD-IPL, *IGLL5* upregulation is

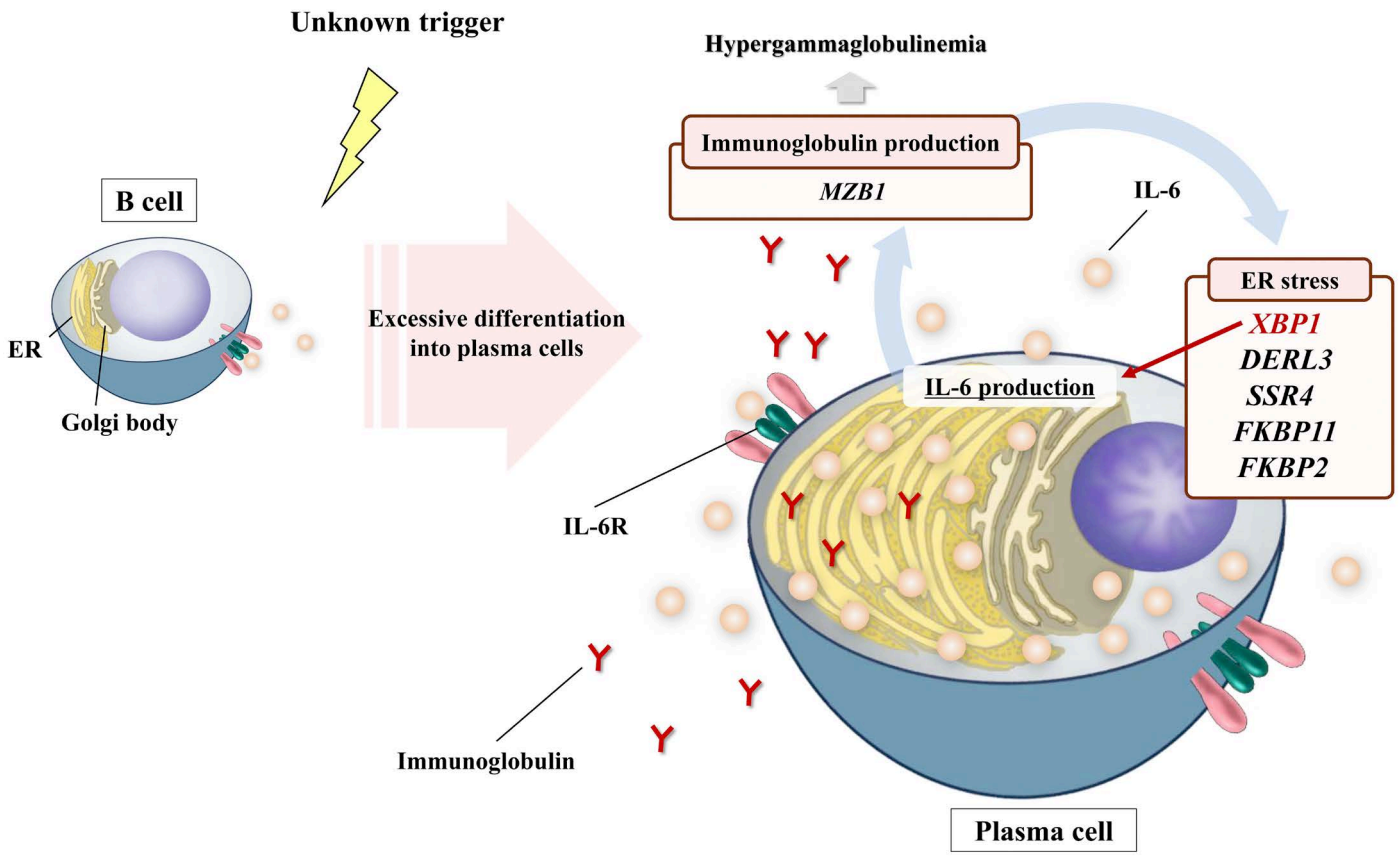

Figure 7. Pathogenesis and gene expression of idiopathic multicentric Castleman disease-idiopathic plasmacytic lymphadenopathy. The pathological hypothesis of idiopathic multicentric Castleman disease with idiopathic plasmacytic lymphadenopathy (iMCF-IPL) is based on the results of immunohistochemistry, *in situ* hybridization, and gene expression analysis. An unknown trigger enhances B-cell differentiation into plasma cells and causes plasma cell proliferation. In this model, plasma cells produce immunoglobulins, resulting in the expansion of the endoplasmic reticulum (ER). Consequently, ER stress-related genes are upregulated, and *XBP1* may be constantly activated, thereby becoming involved in interleukin-6 autocrine production by plasma cells. Immunoglobulin production may upregulate *MZB1* and enhance ER stress. IL-6: interleukin-6; IL-6R: interleukin-6 receptor.

likely attributable to the abundance of plasma cells, as *IGLL5* is located in the immunoglobulin λ locus and is involved in B-cell development.[40] In contrast, the unexpectedly high *IGLL5* expression in iMCD-TAFRO might represent an intriguing paradox, suggesting that different cell types or signals drive *IGLL5* in iMCD-TAFRO. Notably, *IGLL5* expression is also upregulated in multiple myeloma and in tumor-infiltrating immune cells, suggesting a broad role in immune regulation and inflammation.[41,42] One potential hypothesis is that *IGLL5* expression in iMCD-TAFRO might originate from non-plasma cell populations such as activated B cells, dendritic cells, or myeloid-derived suppressor cells, in the setting of widespread endothelial activation and a severe cytokine storm. Future studies should employ single-cell RNA sequencing and spatial transcriptomics to pinpoint the cellular source of *IGLL5* in iMCD and clarify its role in immune dysregulation. These approaches may also determine whether *IGLL5* could serve as a useful biomarker or therapeutic target in specific iMCD subtypes. Several other genes were highly expressed in iMCD-IPL relative to iMCD-TAFRO, including *DERL3, SSR4, FKBP2,* and *FKBP11. DERL3* encodes a Derlin family protein in the ER membrane activated by ER stress.[43] SSR4 encodes a component of the translocation-associated protein (TRAP) complex, which helps translocate proteins across the ER membrane.[44] *FKBP2* and *FKBP11* encode FK506-binding proteins that are upregulated during ER stress; notably, *FKBP11* is induced during *XBP1*-driven differentiation of B cells into plasma cells.[45] The expression patterns support the hypothesis that ER stress-driven IL-6 production by plasma cells is a key feature of iMCD-IPL.

From a clinical standpoint, the present findings underscore the need for subtype-tailored therapy in iMCD. IL-6 blockade remains the first-line treatment, and the results validate its particular importance in iMCD-IPL, in which early anti-IL-6 therapy could interrupt the *XBP1*-driven autocrine IL-6 loop and plasma cell proliferation. However, for patients who have relapsed after or are refractory to IL-6 blockade, there is currently no standard second-line therapy.[8,46] Rituximab, an anti-CD20 B-cell therapy, has a category 2 indication for iMCD in the USA; however, the level of evidence is limited by the retrospective nature of the data and small sample sizes.[46] Given the potential key role of *XBP1* in iMCD-IPL, further studies should explore whether advanced molecular profiling, such as proteomics or gene expression profiling, could guide second-line or later treatment decisions or predict responses to novel targeted therapies.

This study has a few limitations. First, the results of *in situ* hybridization staining were qualitative rather than quantitative because of the limited availability of the lymph node specimens. Second, due to the nature of bulk gene expression analysis, we were unable to identify the cells responsible for expressing each gene. Single-cell gene expression analyses may be beneficial in identifying cells with upregulated genes in iMCD-IPL, including *XBP1* and *MZB1*. In the future, more experiments are required to investigate whether *XBP1* inhibition suppresses IL-6 production. Third, the mechanism of action of IL-6 in vascular endothelial cells was not clear in this study. IL-6 has both trans-signaling and classical signaling pathways, and their effects are different. Since it has been reported that trans-signaling in vascular endothelial cells can amplify inflammatory responses, IL-6 trans-signaling may also be involved in iMCD-TAFRO. To clarify this point, future single-cell analysis is needed. In conclusion, our study elucidates distinct IL-6-producing cells and hypothesized regulatory mechanisms in iMCD subtypes, with *XBP1* potentially playing a pivotal role in IL-6 overproduction in iMCD-IPL. Future studies are warranted to clarify the roles of ER stress and IL-6 and IL-6R in each iMCD subtype. These insights may advance our understanding of iMCD pathogenesis and highlight potential molecular targets for subtype-specific precision therapies.

Disclosures

No conflicts of interest to disclose.

Contributions

AN, MFN and YS conceived the study. AN was responsible for the methodology and formal analysis and wrote the original draft of the manuscript. AN, RY, TH, DE, RC, TI, TK, SM, SO, YK, HU and YT performed the investigations. AN and TH curated data. YN, MFN, MVG, DCF, FvR and YS reviewed and edited the manuscript. MFN and YS supervised the project. All authors read and agreed to the published version of the manuscript.

Funding

This work was partially supported by Japan Society for the Promotion of Science KAKENHI grants (JP 23K1447605 24KK0172, and 25K02476), a Ministry of Health, Labor and Welfare Program grant (JPMH 23FC1025), the Teraoka Scholarship Foundation, and Kurozumi Medical Foundation.

Data-sharing statement

The data that support the findings of this study are available from the corresponding author.

References

1. Fajgenbaum DC, Uldrick TS, Bagg A, et al. International, evidence-based consensus diagnostic criteria for HHV-8-negative/idiopathic multicentric Castleman disease. Blood. 2017;129(12):1646-1657.
2. Wang HW, Pittaluga S, Jaffe ES. Multicentric Castleman disease: where are we now? Semin Diagn Pathol. 2016;33(5):294-306.

3. Nishikori A, Nishimura MF, Nishimura Y, et al. idiopathic plasmacytic lymphadenopathy forms an independent subtype of idiopathic multicentric Castleman disease. Int J Mol Sci. 2022;23(18):10301.
4. Takeuchi K. Idiopathic plasmacytic lymphadenopathy: a conceptual history along with a translation of the original Japanese article published in 1980. J Clin Exp Hematop. 2022;62(2):79-84.
5. Fajgenbaum DC, June CH. Cytokine storm. N Engl J Med. 2020;383(23):2255-2273.
6. Nishikori A, Nishimura MF, Tomida S, et al. Transcriptome analysis of the cytokine storm-related genes among the subtypes of idiopathic multicentric Castleman disease. J Clin Exp Hematop. 2024;64(4):297-306.
7. van Rhee F, Voorhees P, Dispenzieri A, et al. International, evidence-based consensus treatment guidelines for idiopathic multicentric Castleman disease. Blood. 2018;132(20):2115-2124.
8. Fajgenbaum DC, Langan RA, Japp AS, et al. Identifying and targeting pathogenic PI3K/AKT/mTOR signaling in IL-6-blockade-refractory idiopathic multicentric Castleman disease. J Clin Invest. 2019;129(10):4451-4463.
9. Fajgenbaum DC, Wu D, Goodman A, et al. Insufficient evidence exists to use histopathologic subtype to guide treatment of idiopathic multicentric Castleman disease. Am J Hematol. 2020;95(12):1553-1561.
10. Pierson SK, Shenoy S, Oromendia AB, et al. Discovery and validation of a novel subgroup and therapeutic target in idiopathic multicentric Castleman disease. Blood Adv. 2021;5(17):3445-3456.
11. Rubenstein AI, Pierson SK, Shyamsundar S, et al. Immune-mediated thrombocytopenia and IL-6-mediated thrombocytosis observed in idiopathic multicentric Castleman disease. Br J Haematol. 2024;204(3):921-930.
12. Gao YH, Liu YT, Zhang MY, et al. Idiopathic multicentric Castleman disease (iMCD)-idiopathic plasmacytic lymphadenopathy: a distinct subtype of iMCD-not otherwise specified with different clinical features and better survival. Br J Haematol. 2024;204(5):1830-1837.
13. Nishimura MF, Haratake T, Nishimura Y, et al. International consensus histopathological criteria for subtyping idiopathic multicentric Castleman disease based on machine learning analysis. Am J Hematol. 2025;100(9):1502-1512.
14. Tominaga R, Umino K, Honda S, et al. Response to initial treatment with glucocorticoids in TAFRO syndrome and implications for secondary treatment. Int J Hematol. 2025;121(5):658-669.
15. Yu L, Tu M, Cortes J, et al. Clinical and pathological characteristics of HIV- and HHV-8-negative Castleman disease. Blood. 2017;129(12):1658-1668.
16. Mumau MD, Gonzalez MV, Ma C, et al. Identifying and targeting TNF signaling in idiopathic multicentric Castleman's disease. N Engl J Med. 2025;392(6):616-618.
17. Gao YH, Li SY, Dang Y, Duan MH, Zhang L, Li J. Efficacy and safety of orelabrutinib in relapsed/refractory idiopathic multicentric Castleman disease: a single-centre, retrospective study. Br J Haematol. 2025;206(1):152-158.
18. Iwaki N, Gion Y, Kondo E, et al. Elevated serum interferon γ-induced protein 10 kDa is associated with TAFRO syndrome. Sci Rep. 2017;7:42316.
19. Otsuka M, Koga T, Sumiyoshi R, et al. Exploring the clinical diversity of Castleman Disease and TAFRO syndrome: a Japanese multicenter study on lymph node distribution patterns. Am J Hematol. 2025;100(4):592-605.
20. Haratake T, Nishimura MF, Nishikori A, et al. The involvement of PI3K-Akt signaling in the clinical and pathologic findings of iMCD-TAFRO and NOS subtypes. Mod Pathol. 2025;38(1):100782.
21. Lucioni M, Morello G, Cristinelli C, et al. Interleukin-6 transcripts up-regulation in lymph nodes from unicentric and multicentric Castleman disease. EJHaem. 2024;5(6):1182-1189.
22. Horna P, King RL, Jevremovic D, Fajgenbaum DC, Dispenzieri A. The lymph node transcriptome of unicentric and idiopathic multicentric Castleman disease. Haematologica. 2023;108(1):207-218.
23. Chan JY, Loh JW, Lim JQ, et al. Single-cell landscape of idiopathic multicentric Castleman disease in identical twins. Blood. 2024;143(18):1837-1844.
24. Yin X, Liu Y, Ding S, et al. IFN-γ promotes the progression of iMCD by activating inflammatory monocytes. Blood. 2025;146(1):76-88.
25. Satou A, Notohara K, Zen Y, et al. Clinicopathological differential diagnosis of IgG4-related disease: a historical overview and a proposal of the criteria for excluding mimickers of IgG4-related disease. Pathol Int. 2020;70(7):391-402.
26. Nishikori A, Nishimura MF, Fajgenbaum DC, et al. Diagnostic challenges of the idiopathic plasmacytic lymphadenopathy (IPL) subtype of idiopathic multicentric Castleman disease (iMCD): factors to differentiate from IgG4-related disease. J Clin Pathol. 2025;79(1):43-49.
27. Mori S, Mohri N. [Clinicopathological analysis of systemic nodal plasmacytosis with severe polyclonal hyperimmunoglobulinemia]. Proc Jpn Soc Pathol. 1978;67:252-253.
28. Kojima M, Nakamura N, Tsukamoto N, et al. Clinical implications of idiopathic multicentric Castleman disease among Japanese: a report of 28 cases. Int J Surg Pathol. 2008;16(4):391-398.
29. Zhang L, Dong YJ, Peng HL, et al. A national, multicenter, retrospective study of Castleman disease in China implementing CDCN criteria. Lancet Reg Health West Pac. 2023;34:100720.
30. Masaki Y, Kawabata H, Takai K, et al. 2019 Updated diagnostic criteria and disease severity classification for TAFRO syndrome. Int J Hematol. 2020;111(1):155-158.
31. Nishimura Y, Fajgenbaum DC, Pierson SK, et al. Validated international definition of the thrombocytopenia, anasarca, fever, reticulin fibrosis, renal insufficiency, and organomegaly clinical subtype (TAFRO) of idiopathic multicentric Castleman disease. Am J Hematol. 2021;96(10):1241-1252.
32. Newman AM, Steen CB, Liu CL, et al. Determining cell type abundance and expression from bulk tissues with digital cytometry. Nat Biotechnol. 2019;37(7):773-782.
33. van Diest PJ, van Dam P, Henzen-Logmans SC, et al. A scoring system for immunohistochemical staining: consensus report of the task force for basic research of the EORTC-GCCG. European Organization for Research and Treatment of Cancer-Gynaecological Cancer Cooperative Group. J Clin Pathol. 1997;50(10):801-804.
34. Abu-Eid R, Ward FJ. Targeting the PI3K/Akt/mTOR pathway: a therapeutic strategy in COVID-19 patients. Immunol Lett. 2021;240:1-8.
35. Karar J, Maity A. PI3K/AKT/mTOR pathway in angiogenesis. Front Mol Neurosci. 2011;4:51.
36. Iwakoshi NN, Lee AH, Glimcher LH. The X-box binding protein-1 transcription factor is required for plasma cell differentiation and the unfolded protein response. Immunol Rev. 2003;194:29-38.
37. Tang TF, Chan YT, Cheong HC, et al. Regulatory network of BLIMP1, IRF4, and XBP1 triad in plasmacytic differentiation and multiple myeloma pathogenesis. Cell Immunol.

2022;380:104594.
38. Zeng L, Xiao Q, Chen M, et al. Vascular endothelial cell growth-activated XBP1 splicing in endothelial cells is crucial for angiogenesis. Circulation. 2013;127(16):1712-1722.
39. Reimold AM, Iwakoshi NN, Manis J, et al. Plasma cell differentiation requires the transcription factor XBP-1. Nature. 2001;412(6844):300-307.
40. Lundmark A, Gerasimcik N, Båge T, et al. Gene expression profiling of periodontitis-affected gingival tissue by spatial transcriptomics. Sci Rep. 2018;8(1):9370.
41. White BS, Lanc I, O'Neal J, et al. A multiple myeloma-specific capture sequencing platform discovers novel translocations and frequent, risk-associated point mutations in IGLL5. Blood Cancer J. 2018;8(3):35.
42. Xia ZN, Wang XY, Cai LC, Jian WG, Zhang C. IGLL5 is correlated with tumor-infiltrating immune cells in clear cell renal cell carcinoma. FEBS Open Bio. 2021;11(3):898-910.
43. Lin L, Lin G, Lin H, et al. Integrated profiling of endoplasmic reticulum stress-related DERL3 in the prognostic and immune features of lung adenocarcinoma. Front Immunol. 2022;13:906420.
44. Losfeld ME, Ng BG, Kircher M, et al. A new congenital disorder of glycosylation caused by a mutation in SSR4, the signal sequence receptor 4 protein of the TRAP complex. Hum Mol Genet. 2014;23(6):1602-1605.
45. Hoefner C, Bryde TH, Pihl C, et al. FK506-binding protein 2 participates in proinsulin folding. Biomolecules. 2023;13(1):152.
46. Lang E, van Rhee F. Idiopathic multicentric Castleman disease: an update in diagnosis and treatment advances. Blood Rev. 2024;64:101161.